Fibres and soils: A route towards modelling of root-soil systems

N.B. When citing this work, cite the original published paper.

(article starts on next page)

IS-Cambridge

Fibres and soils: A route towards modelling of root-soil systems

David Muir Wood[a,b,c,*], Andrea Diambra[c], Erdin Ibraim[c]

[a]*Institutionen för Bygg-och Miljöteknik, Chalmers Tekniska Högskola, Göteborg, Sweden*
[b]*Division of Civil Engineering, Fulton Building, University of Dundee, United Kingdom*
[c]*Department of Civil Engineering, University of Bristol, United Kingdom*

Abstract

The addition of flexible fibres to granular, cohesionless soils, has a marked influence on the stress:strain and volumetric response. Experimental observations provide inspiration for the development of continuum models for the mechanical, pre-failure behaviour of these fibre/soil mixtures. Such generic models and the deduced mechanisms of response should be applicable to other combinations of soils and flexible fibres such as plant roots. Two features are particularly important: the distribution of the orientations of fibres (no method of preparation produces an isotropic distribution) and the allowance for the volume of void space not only occupied, but also influenced, by the presence of the fibres.

A simple shear element is used as a quasi-one-dimensional demonstrator platform for the presentation of the continuum constitutive model. Such an element represents a familiar configuration in which phenomena, such as dilation and friction, can be directly observed. A basic constitutive model for sand is adapted to this simple shear element; the fibres are added as a separate component able to withstand tension but without flexural stiffness. As the soil-fibre mixture deforms, the straining of the soil generates stresses in favourably oriented fibres. The model is used to clarify some aspects of the response of the fibre-soil mixtures: the influence of fibres on the volumetric behaviour; the existence and nature of asymptotic states; and the stress–dilatancy relationship.
© 2016 The Japanese Geotechnical Society. Production and hosting by Elsevier B.V. This is an open access article under the CC BY-NC-ND license (http://creativecommons.org/licenses/by-nc-nd/4.0/).

Keywords: Fibres; Cohesionless soils; Ground improvement; Constitutive model

1. Introduction

It has been known, qualitatively, for many centuries that the presence of vegetation has beneficial effects on the stability and deformations of slopes through the reinforcing effect of the roots on the soil through which they are growing (Wu et al., 1988; Reubens et al., 2007). Roots, subject to the vagaries of nature, present challenges for testing and modelling. The laboratory observations presented here relate to the behaviour of cohesionless soil (sand) mixed with flexible polypropylene fibres which will be somewhat similar to the behaviour of soils containing actual plant roots. We are concerned in the present study with only the mechanical and not the hydrological effects. However, provided a model is available to describe the behaviour of the soil (saturated or unsaturated), in the absence of fibres/roots, the effect of the fibres can then be added in a systematic way.

There have been several studies of the influence of flexible fibres on the strength of soils. Failure criteria have been developed using force equilibrium considerations in a localised shear band (Jewell and Wroth, 1987; Maher and Gray, 1990; Ranjan et al., 1996); energy-based homogenisation approaches (Michałowski and Čermák, 2002); or the discrete superposition of the sand and fibre effects (Zornberg, 2002). Quantitative

*Corresponding author.
  E-mail address: d.muirwood@dundee.ac.uk (D. Muir Wood).

modelling of the pre-failure behaviour of fibre-soil mixtures has received less attention, and proposed models have dealt with the elastic behaviour of the material (Ding and Hargrove, 2006) or have been applied to soils reinforced with continuous thread (Texsol) (Villard et al., 1990; di Prisco and Nova, 1993). The two-dimensional DEM (Distinct Element Method) has been used to investigate the micromechanical aspects of the interaction between grains and fibres and the distribution of the tensile stresses mobilised in the fibres (Ibraim et al., 2006; Ibraim and Maeda, 2007).

Our modelling environment takes the form of an infinitesimal simple shear element (like an element at the centre of a direct shear box) (Fig. 1). There are several reasons for taking this elemental approach (Muir Wood, 2009): the direct shear box is a particularly simple pedagogic device which shows students or other users exactly what is happening in terms of linked volumetric and shearing deformations; the simple shear element is directly applicable to the deformation and sliding of a long slope and also to the propagation of shear waves in an earthquake; and there have been a number of developments in constitutive modelling over the past few decades which have endeavoured to include the influences of fabric anisotropy and the history of loading or deformation by considering the overall response to be the summation of responses of a series of shear elements distributed over all possible orientations. The microstructural model of Calladine (1971) applies to soils a framework suggested by Batdorf and Budiansky (1949) for metals, and this approach has been rediscovered in multi-laminate modelling (Pande and Sharma, 1983) and in the models of Chang and Hicher (2005).

The modelling framework has been described by Diambra et al. (2013) and Muir Wood et al. (2014); it will be summarised briefly here and used to illustrate some aspects of the response of fibre-soil mixtures: the influence of fibres on the volumetric behaviour; the existence and nature of asymptotic states; and the stress-dilatancy relationship for the mixtures.

2. Experimental observations

Inspiration for the modelling has come from an extensive experimental study on the behaviour of mixtures of Hostun sand ($d_{50}=0.38$ mm, $C_u=1.9$) with short flexible polypropylene fibres (length 35 mm, diameter 0.1 mm) (Ibraim and Fourmont, 2007; Diambra et al., 2010). It is hypothesised that the behaviour of soil containing flexible plant roots will be broadly subject to the same characteristics of mechanical interaction. Fibres can be mixed with the soil in carefully monitored proportions: attention to detail of the sample preparation techniques encourages the formation of some-what repeatable samples. On the other hand roots grow through the soil, feeling their way between the soil particles or the packets of particles, and developing bonding by a process of cavity expansion as the root expands within its chosen tortuous void space and develops restraining confinement stresses as it grows. The detailed fabric of soil root mixtures is expected to be more variable, whether in the laboratory or in the field, so the tests on polypropylene fibre mixtures are consequently more useful for the initial development of constitutive models.

Direct shear tests with constant vertical stress $\sigma_z=55.3$ kPa (Fig. 2) and with values of specific volume between 1.8 and 2.0 (corresponding to relative densities of approximately 60% and 0%) show increased shear stress and increased dilatancy as a result of the addition of flexible fibres (Ibraim and Fourmont, 2007). Fig. 2a, b, d, e show the variation in shear stress and vertical displacement or volume change (u_z) with horizontal displacement u_x. The rate of change in vertical displacement with horizontal displacement, equivalent to an angle of dilation $\tan\psi=-\delta u_z/\delta u_x$, is plotted against externally measured values of mobilised friction τ/σ_z in Fig. 2c, f. The effect of fibres on dilatancy is confirmed in undrained triaxial compression tests on loose fibre-sand mixtures which show reduced and even negative pore pressures; the presence of fibres produces a significant reduction in liquefaction potential (Ibraim et al., 2010a; Diambra et al., 2011).
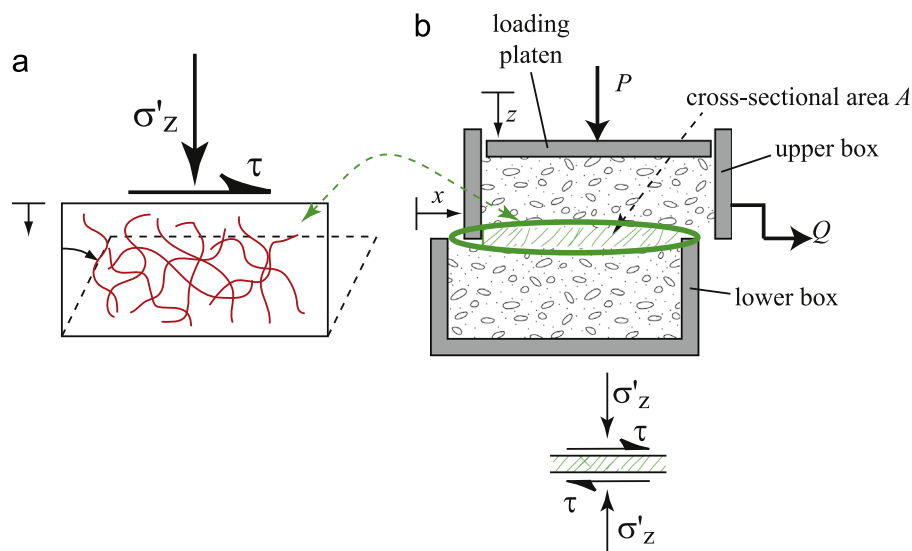

Fig. 1. (a) Simple shear element of soil with fibres; (b) corresponding to central region of shear box.
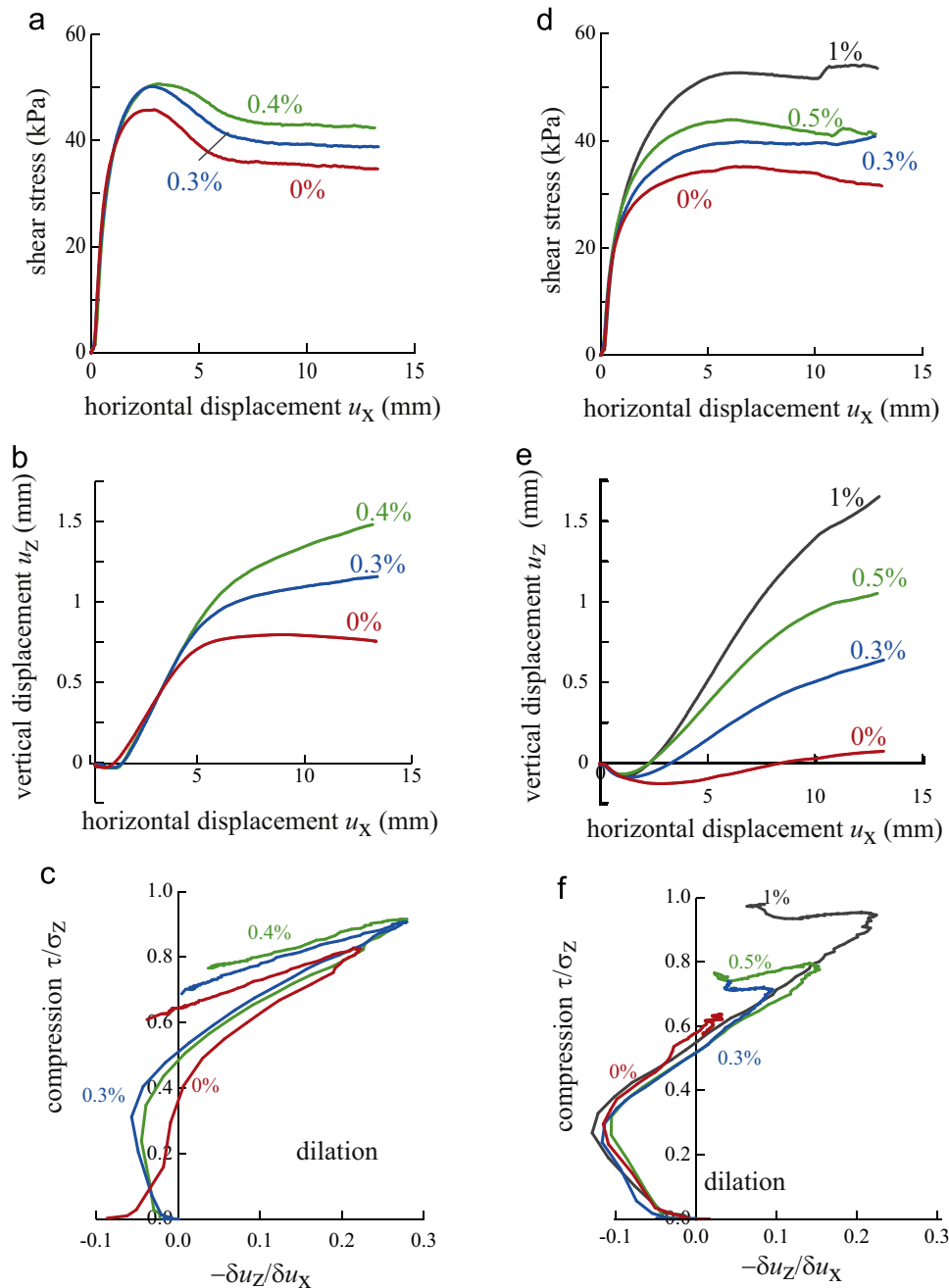
Fig. 2. Direct shear box tests on fibre/soil mixtures: sand specific volume: a, b, c. $v_o = 1.8$; d, e, f. $v_o = 2.0$; a, d: mobilised friction and shear displacement; b, e: vertical displacement and shear displacement; c, f: dilatancy $\delta u_z/\delta u_x$ and externally measured mobilised friction τ/σ_z; $\sigma_z = 55.3$ kPa (Ibraim and Fourmont, 2007).

However, not all published papers report increased dilatancy (Heineck et al., 2005). This apparent contradiction can be linked to the different modelling assumptions implicit in the experimental approach employed for the comparison of unreinforced and reinforced sand samples. It will be discussed in a later section of this paper.

3. Model for fibre/sand mixtures

The soil is seen as the *active* component and the fibres as the *reactive* component. A series of hypotheses are introduced to describe the interactive behaviour (Diambra et al., 2013):

- The sand matrix in the presence of fibres can be described by the same model as the unreinforced soil.
- Tensile strains in the soil try to stretch the fibres. Interaction between fibres and soil requires some mechanical bond or anchorage.
- Fibres are treated as forces with orientation and not as a continuous superimposed material. They have tensile stiffness and strength, but negligible compression or flexural stiffness or strength.
- Stretched fibres try to resist extension, and thus, tend to increase the normal stress on the soil, but also contribute directly to the shear stress.

- In their interaction with the soil, as the strains increase, the fibres may pull out of the soil or may reach their tensile strength and snap.
- Allowance must be made for the presence of fibres when calculating the operational specific volume or void ratio of the soil.

The first three hypotheses relate to the two separate materials: soil and fibres. The last three hypotheses relate to the interaction between the fibres and the surrounding soil. This approach to modelling is described as the 'Discrete framework' by Li and Zornberg (2013).

3.1. Severn-Trent sand

The description of the fibre-soil interaction can be combined with any model for the soil itself (Diambra and Ibraim, 2014). Severn-Trent sand is an extended Mohr–Coulomb frictional model in which the strength and dilatancy vary as a function of the distance of the current state of the soil from asymptotic critical states (Gajo and Muir Wood, 1999a, 1999b). This underpinning model for the sand is built around the interaction of four components (Fig. 3). We will need to refer to elements of this model in subsequent discussions.

When subjected to monotonic shearing, the sand reaches eventual asymptotic critical states in which shearing can continue with no further change in effective stress, density or fabric (on average) (Fig. 3a). In order to ensure that the critical state line does not suggest unreasonable values for void ratio e or specific volume v at very low or very high stresses, the following form proposed by Gudehus (1997) has been used:

$$v_c = v_{min} + \Delta v \exp\left[-\left(\frac{\sigma_z}{\sigma_{ref}}\right)^{\beta}\right] \qquad (1)$$

where $\Delta v = v_{max} - v_{min}$ defines the range in values of specific volume $v = 1 + e$; σ_{ref} is a reference stress; and β is a soil parameter. A 'state parameter', ψ, (Wroth and Bassett, 1965; Been and Jefferies, 1985) can be defined which encapsulates the volumetric distance of the current state of the sand (σ_z and v) from the critical state condition for the same effective stress. The sand has a rather clear feeling for the change in volumetric packing required to bring it to this asymptotic state.

The current strength of this frictional soil is not a constant, but depends on density and stress through the current value of the state parameter (Fig. 3b). Loose sands, with current specific volume greater than the critical state specific volume ($\psi > 0$), show low current strength; dense sands, with current specific volume below the critical state specific volume ($\psi < 0$), show high current strength.

The plastic hardening of the soil is purely distortional, resulting from the rearrangement of the soil particles; the plastic stiffness falls steadily as the mobilised friction increases towards the currently available strength (Fig. 3c). The plastic hardening is described by a monotonic relationship. The flow rule linking plastic volumetric dilation with plastic distortion (Fig. 3d) provides a feedback link.

The operation of the model can be simply described. Increments in (plastic) distortional strain lead to increases in the mobilisation of the *currently available* strength, (Fig. 3c). The flow rule requires there to be plastic volumetric strains accompanying the distortional strains (Fig. 3d). The resulting change in volume moves the state of the sand closer to the critical state (from above or below) (Fig. 3a). The resulting change in state parameter leads to a change in the *available* strength (Fig. 3b) so that the distortional hardening is moving the state of the soil towards a moving target. The close interlocking of the elements of the model (Fig. 3) ensures that, with continuing monotonic shearing, the state of
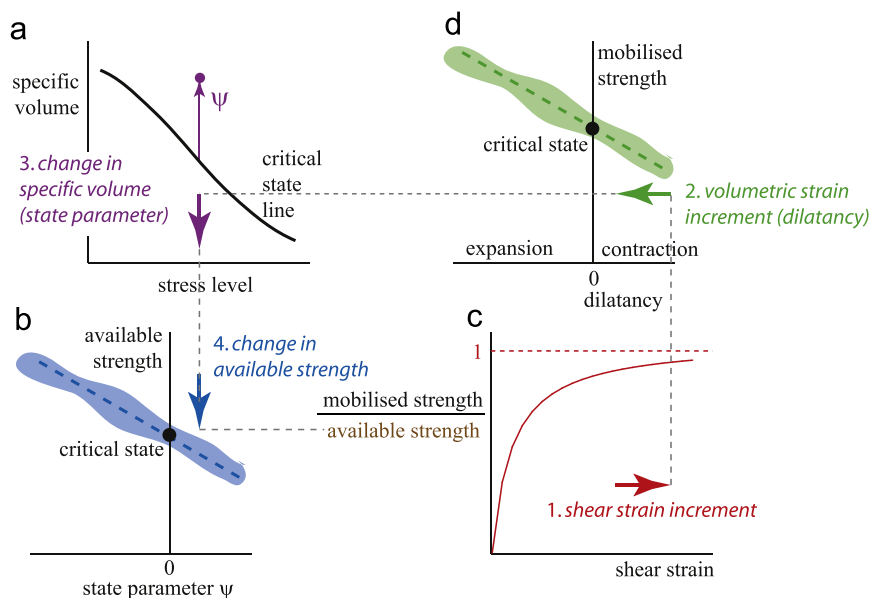

Fig. 3. Four elements of Severn-Trent sand model: (a) critical state line and state parameter; (b) strength dependent on state parameter; (c) monotonic hardening relationship; (d) stress:dilatancy relationship.

the sand heads for an asymptotic critical state. The combination of these four components produces a satisfyingly rich range of simulated responses with a rather small number of soil parameters.

3.2. Contribution of fibres

Tensile strains in the soil try to stretch any fibres whose orientation engages with the tensile sector of the Mohr circle of strain increment (Fig. 4). The simple shear element has two degrees of strain increment freedom: vertical or volumetric strain and shear strain. The horizontal direction is always inextensional, such that the Mohr circle of strain increment must intersect (or, in the limit, touch) the shear strain axis $\delta\varepsilon=0$. This Mohr circle defines the range of orientations within the sample for which the strain increment has a tensile component (Fig. 4a, b, d). There will always be some such orientations except when the sample is being subjected to pure (one-dimensional) compression (Fig. 4c). For shearing at constant volume, fibres with orientations between 0 and $\pi/2$ to the horizontal (in the direction opposite to the shearing) will develop tensile strains (Fig. 4d).

It is obviously necessary to know the actual distribution of the orientation of fibres in the sample that is to be simulated. Typical techniques for the preparation of fibre/soil mixtures do not produce random distributions of fibre orientation (Diambra et al., 2007): moist tamping inevitably leaves the fibres in a somewhat sub-horizontal orientation (Michałowski and Čermák, 2003). Information is needed concerning both the *spatial distribution of fibres* and the distribution of *fibre orientations*. A homogeneous spatial distribution is a reasonable experimental goal, whereas the distribution of orientations is an outcome which must be known even if it cannot be precisely controlled.

The same information is required for plant roots: the distribution and orientation of the flexible elements which may well have different diameters. Plants can be divided into two groups: 'oligorhizoid' dicotyledons have a few rather substantial roots (such as mustard, Fig. 5b); monocotyledons, such as grasses, tend to be more 'polyrhizoid' in character (Fig. 5a) having more finer roots which are much more randomly distributed. Such polyrhizoid species are more obviously suited to a continuum approach to modelling. Polyrhizoid plant species, forming an interlocking cluster of reinforcement, will provide an apparent cohesion in near surface soils for which the frictional strength is very low. They are obvious candidates for improving slope stability through the enhancement of the mechanical properties. The topology or architecture of plant roots is more complicated than that of uniform identical flexible fibres. However, there exist compendia of immaculate drawings of roots for different species (Kutschera et al., 1960–2009) which can provide some initial guidance.

The outcome of these direct measurements, or estimates, is a probability density function $Np_\theta\delta\theta$ describing the proportion of the total number N of fibres (of different diameters for roots) within the angular sector $\delta\theta$ with orientation θ crossing the unit area of the simple shear sample (Fig. 6a).

A tensile test on a polypropylene fibre is shown in Fig. 6c and tensile tests on roots of vetch are shown in Fig. 5c. As a
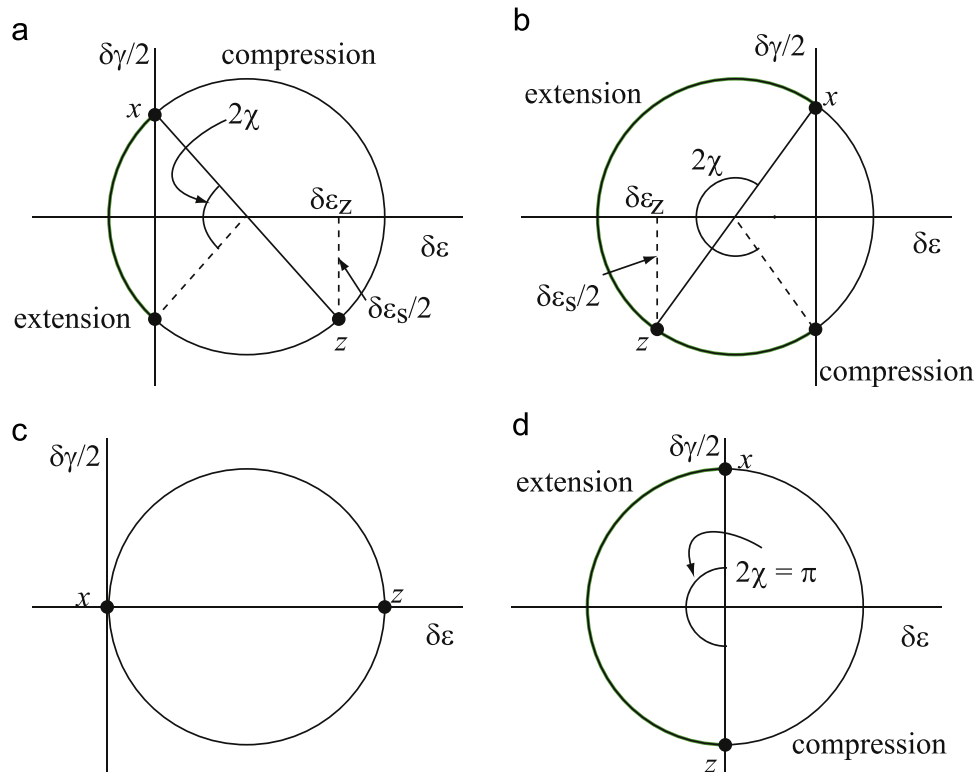

Fig. 4. Mohr's circle of strain increment for simple shear sample: (a) shearing with volumetric compression $\delta\varepsilon_z > 0$; (b) shearing with volumetric expansion $\delta\varepsilon_z < 0$; (c) one-dimensional compression; (d) constant volume shearing $\delta\varepsilon_z = 0$.

first assumption, we will assume that the response of the polypropylene fibres is linear elastic until plastic ductile failure is reached at a yield strain ε_{fy} and subsequent breakage strain ε_{fb}. We assume a Young's modulus E_f to convert the fibre strain to an axial force in the elastic region $\delta P = \delta\sigma_{af}a_f = E_f a_f \delta\varepsilon_f$ along the fibre of cross-sectional area a_f. If $\varepsilon_f > \varepsilon_{fy}$, then $\delta P = 0$.

Stressed fibres contribute vertical and horizontal components of force to the stress state on the horizontal plane of the simple shear soil element (Fig. 6b). Fibres try to resist stretching because they are anchored in the soil by the clamping forces of the soil particles along the length of the fibres. Consequently, fibres will increase the normal stress $\delta\sigma_{zf}$;

fibres with orientation $\theta < \pi/2$ will also contribute to the shearing resistance of the composite element $\delta\tau_f$.

$$\delta\sigma_{zf} = Np_\theta E_f a_f \delta\varepsilon_f \sin\theta \quad \delta\tau_f = Np_\theta E_f a_f \delta\varepsilon_f \cos\theta \quad (2)$$

Stretched fibres having orientations $\theta > \pi/2$ (with tensile strain increment range $2\chi > \pi$ (Fig. 4b) will reduce the shearing resistance slightly while still boosting the normal stress.

Strains develop in the fibres because of the strains that occur in the soil around the fibres. However, the fibre-grain interaction is rather complex. The fibres take an erratic route between the soil grains (Lirer et al., 2011; Heineck et al., 2005; Consoli et al., 2005), and the axial strains usually vary along the length of the fibres. Shear distortions at the interface between the two materials and the end-effects occur in fibre-reinforced composites (Hull and Clyne, 1996). These phenomena can be included in a continuum modelling approach by simply introducing a mismatch between the strains in the fibre and the soil (Diambra and Ibraim, 2015):

$$\delta\varepsilon_f = f_m \delta\varepsilon_m \quad (3)$$

where $\delta\varepsilon_f$ and $\delta\varepsilon_m$ are the strain increments in the fibre and the soil matrix, respectively, and $f_m < 1$ is a strain 'mismatch' factor. Using appropriate modification of the shear lag theory for composite materials (Cox, 1952), Diambra and Ibraim (2015) derived a complete expression for f_m which explicitly considers the geometry of the fibre and grains, fibre stiffness, global stress level, soil density, and the non-linearity of soil behaviour. Here we have used a simpler expression for f_m which accounts for the fundamental effect of the stress level in the soil, σ_{zs}, which will be greater than the externally applied stress because of the extra stress generated by the stretched fibres:

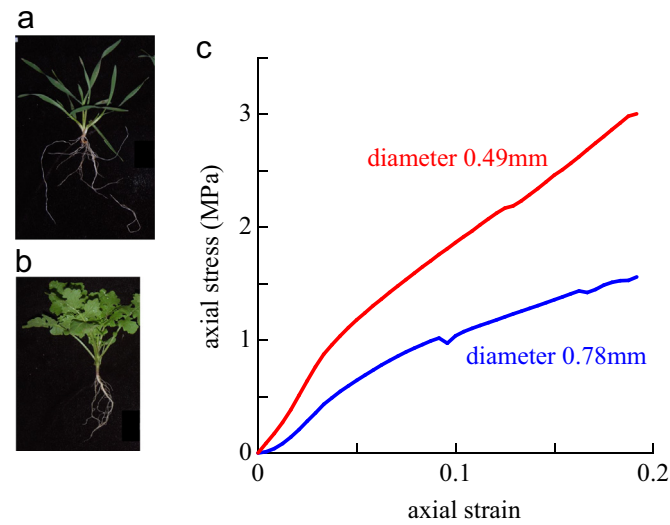$$f_m = 1 - \lambda exp\left[-\left(\frac{\sigma_{zs}}{\sigma_r}\right)\right] \quad (4)$$

Fig. 5. Root architecture for (a) rye grass *Lolium mul. Westerwoldicum*; (b) mustard *Brassica nigra*; (c) tensile tests on plant roots of vetch (*Vicia sativa*) (Liang, 2016).
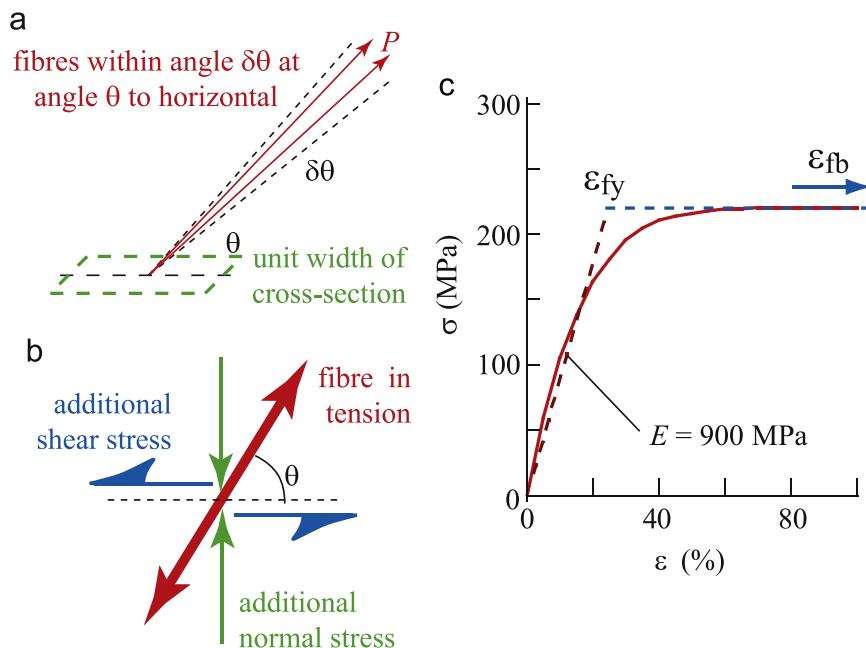

Fig. 6. (a) Orientation and distribution of fibres and (b) contribution to normal stress and shear stress; (c) tensile test on polypropylene fibre.

where σ_r is a reference stress and λ controls the degree of mismatch for a given stress level. The mismatch between the soil and the matrix decreases as the surrounding stress level increases (Diambra and Ibraim, 2015). The incremental force in the fibre is then $\delta P = E_f a_f \delta\varepsilon_f$: the strain mismatch reduces the apparent fibre stiffness.

4. Simulation and discussion

A set of comparisons of simulated and laboratory direct shear tests on fibre-sand mixtures, using a single set of soil parameters, (and with fibre orientations uniformly distributed) is shown in Fig. 7. The simulations are described in terms of strains, the direct shear tests are reported in terms of displacements, but the general concordance between the observations and the simulations is good.

4.1. Volumetric interaction and fibrespace

There are various ways in which the volumetric packing of sand can be described in the presence of fibres; and the

preparation technique, applied with the intention of preparing comparable samples with different fibre contents, will itself make some assumptions about what constitutes an appropriate measure of packing.

The fibres have volume V_f, the soil particles have volume V_s and there are voids with volume V_v. Let us suppose that the fibres themselves require some volume of surrounding voids (Diambra et al., 2010) - in other words that they steal some void ratios from the soil in order to create their own fibrespace (Fig. 8). The volume of fibrespace might be somehow linked to the surface area of the fibres (Muir Wood, 2012). The total volume of voids is then divided into V_{vf} associated with the fibres and V_{vs} associated with the soil. The specific volume of the fibres in the fibrespace is

$$v_f = \frac{V_{vf} + V_f}{V_f} \tag{5}$$

The volume proportion for the fibres is $\rho = V_f/(V_f + V_s)$ and the volume ratio is $V_f/V_s = \rho/(1-\rho)$. Samples will usually be prepared by mass: the proportion of masses $f = M_f/(M_f + M_s)$.
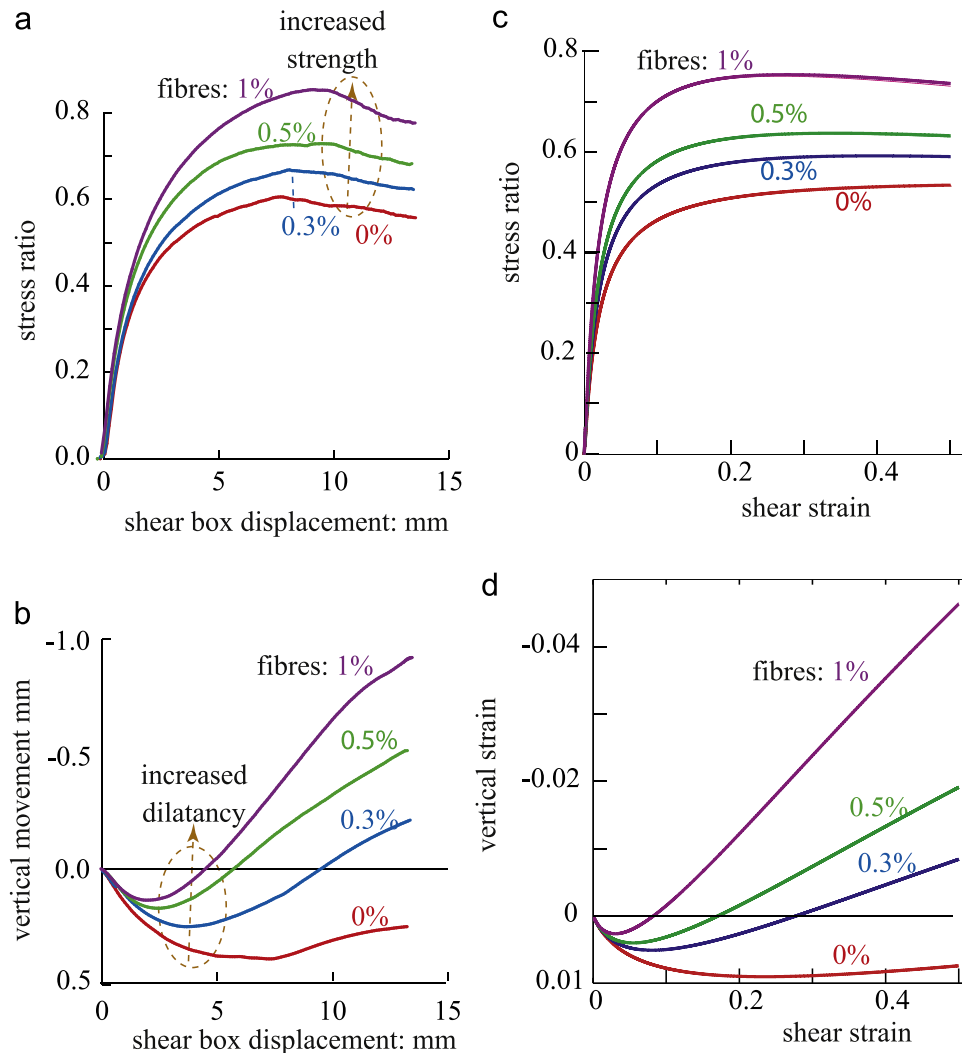

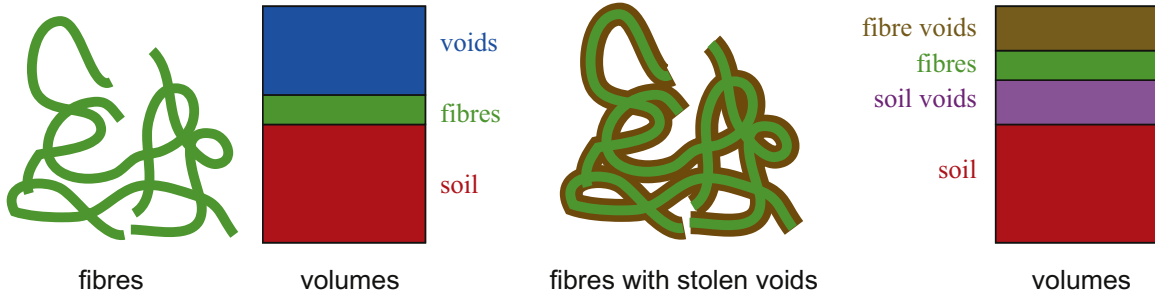Fig. 7. Direct shear tests on fibre-sand mixtures: (a, b) observation; (c, d) simulation.

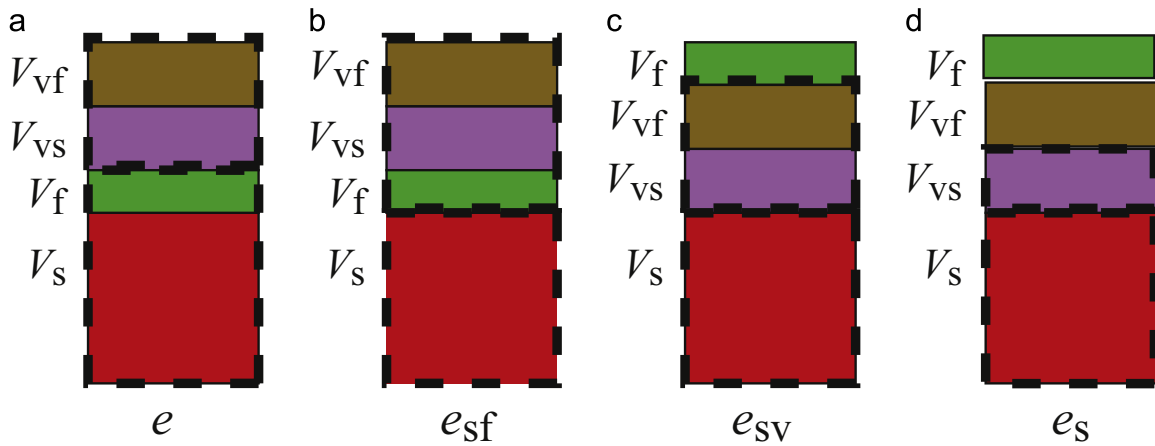Fig. 8. Fibres stealing void from sand to create fibrespace.

Fig. 9. Alternative definitions of void ratio.

With specific gravity G_f and $G_s = G_f/k_G$ for fibres and soil particles:

$$f = \frac{k_G\rho}{1-\rho(1-k_G)} \qquad (6)$$

so that, if $k_G \sim 1/3$, and $\rho \ll 1, f \sim \rho/3$.

The void ratio is e, the ratio of the volume of all voids to the volume of all solids (particles and fibres) (Fig. 9a):

$$e = \frac{V_v}{V_f+V_s} = \frac{V_{vs}+V_{vf}}{V_f+V_s} \rightarrow v = 1+e \qquad (7)$$

The volume of fibres is small and they hardly provide a continuous load-bearing phase. A generous void ratio can then be defined, treating everything apart from the soil particles themselves as void space, e_{sf} (Fig. 9b):

$$e_{sf} = \frac{V_v+V_f}{V_s} = \frac{e+\rho}{1-\rho} \rightarrow v_{sf} = \frac{v}{1-\rho} \qquad (8)$$

If we associate all the voids with the soil particles, but leave the volume of fibres with no attached voids, there is an intermediate void ratio e_{sv} (Fig. 9c):

$$e_{sv} = \frac{V_v}{V_s} = \frac{e}{1-\rho} \rightarrow v_{sv} = \frac{v-\rho}{1-\rho} \qquad (9)$$

If we regard the voids contained in the fibrespace as inalienable, then we can define a soil void ratio, e_s (Fig. 9d) as

$$e_s = \frac{V_{vs}}{V_s} = \frac{e+(1-v_f)\rho}{1-\rho} \rightarrow v_s = \frac{v-v_f\rho}{1-\rho} \qquad (10)$$

These various definitions of void ratio and specific volume are compared in Fig. 10a for $v=1.6$ and $v_f=3$.

An immediate illustration of the effect of this stolen void ratio or fibrespace is provided by the results of the procedure adopted for preparation of the fibre-sand mixtures (Fig. 10b) (Ibraim et al., 2012; Ibraim and Fourmont, 2007). For a given amount of tamping effort, the final density of packing decreases as the fibre content increases. One-dimensional compression linked with tamping produces only compression direct strain increments overall (Fig. 4c), so that there is no obvious possibility at the 'system' level of fibres being stretched by tensile strain increments in order to influence compaction. However, at the particle level, there may be some mechanical interaction with the fibres because of local fabric changes (Consoli et al., 2005; Ibraim et al., 2006; Diambra and Ibraim, 2015). If we suppose that the soil always reaches the same density at the conclusion of tamping, we can then ascribe the lower overall density to the need to include the fibrespace. Analysis of the compaction produces fibrespace specific volumes of $v_{sf} \sim 5$–10. These may seem a little high, but with this magnitude the simulations become reasonable.
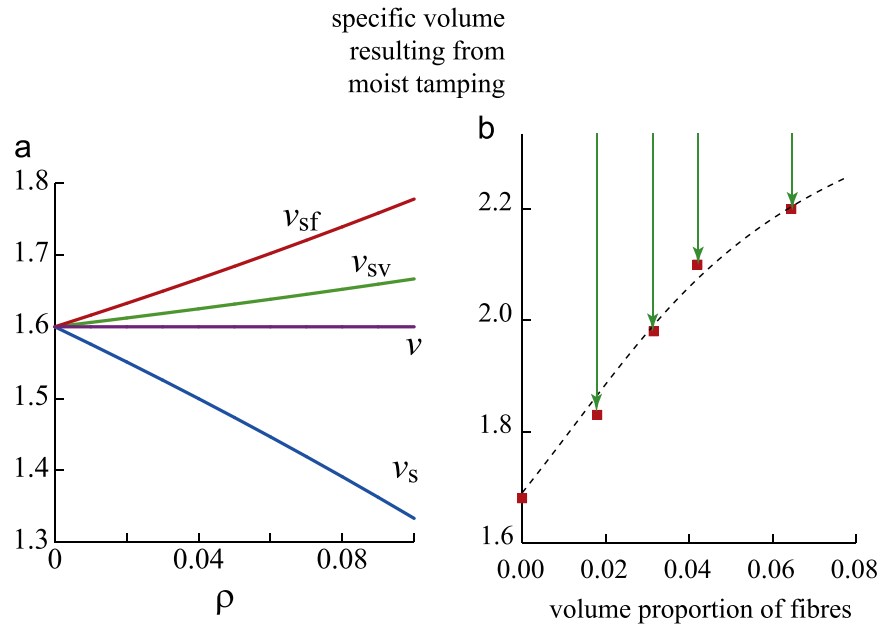
Fig. 10. (a) Alternative definitions of specific volume ($v=1.6$, $v_f=3$); (b) effect of fibre content on specific volume obtained by moist tamping sample preparation.
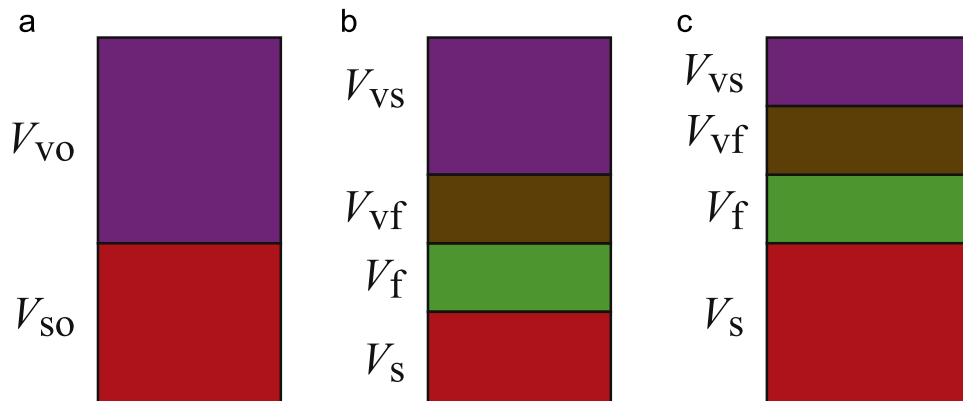

Fig. 11. Alternative strategies for preparation of soil/fibre mixtures: (a) unreinforced soil; (b) fibres replace soil (overall volume constant); (c) fibres replace void (overall volume constant).

Is it possible to choose the initial density of the soil-fibre specimens to guarantee a direct comparability of the response? Two strategies have been adopted for the preparation of fibre-soil mixtures (Fig. 11) (v_o and ρ are the specific volume of the plain sand and the proportion of fibres by volume of fibres plus soil):

1. Some of the volume of soil particles is replaced by fibres so that the specific volume of the mixture matches the specific volume of the plain sand $v=v_o$ (Fig. 11b) (Silva dos Santos et al., 2010; Michałowski and Čermák, 2003; Heineck et al., 2005) [$v=v_o$, $v_{sf}=v_o/(1-\rho)$, $v_{sv}=(v_o-\rho)/(1-\rho)$; $v_s=(v_o-v_f\rho)/(1-\rho)$].
2. The volume of sand is kept constant and the addition of fibres replaces some of the voids (Fig. 11c) so that the specific volume $v_{sf}=v_o$ (Fig. 9b) (Diambra et al., 2010; Ibraim et al., 2010a) [$v=v_o(1-\rho)$, $v_{sf}=v_o$, $v_{sv}=v_o-\rho/(1-\rho)$, $v_s=v_o-v_f\rho/(1-\rho)$]. This is the strategy adopted for the tests shown in Fig. 7a, b.

Evidently $v_o > v_o(1-\rho)-\rho$ and the second strategy will produce denser samples which will show greater dilation, even before the fibrespace of fibres and voids is removed from the calculation of effective densities. This is confirmed in the simulations in Fig. 12.

A simple conclusion is that it is meaningless to say that 'the addition of fibres increases (or decreases) dilatancy', because such a statement can only be made in the context of a complete description of the procedure for preparing, testing and modelling the soil-fibre mixtures. Properly contextualised, the observation becomes another element of the dataset to incorporate into the modelling.

4.2. Asymptotic states and stress-dilatancy

When sheared continuously, soils reach an asymptotic state in which all aspects of the definition of the state reach stationary values. The classical asymptotic critical state was
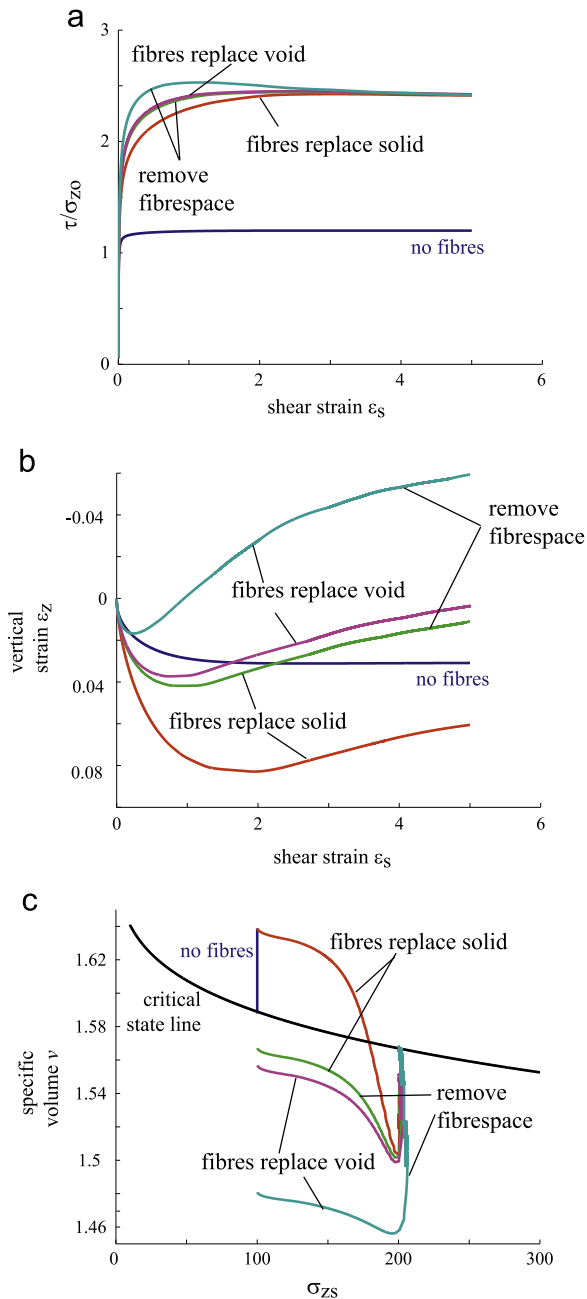
Fig. 12. Simulations of shearing with constant vertical stress $\sigma_z = \sigma_{zo}$; initial densities chosen according to different preparation strategies: fibres replace soil particles or fibres replace voids; fibrespace removed or not removed before calculating effective density; (a) shear stress τ/σ_{zo} and shear strain ε_s; (b) vertical strain ε_z and shear strain ε_s; (c) specific volume v_s of soil and vertical stress experienced by soil σ_{zs} ($v_f = 3$, $\rho = 0.03$).

concerned only with the stationary values of stresses and density (void ratio) (Roscoe et al., 1958). However, a properly asymptotic state requires that the fabric, the particle grading and the particle shape have also reached steady conditions. For the fibre-soil mixtures, both the soil and the fibres (in their interaction with the soil) in our infinitesimal simple shear element must have reached a steady state. For the soil, the critical state will be the same as that of the soil tested on its own. For the fibre-sand mixtures, we can envisage two possible interactive asymptotic states (Fig. 13). The limiting tensile force that can be transmitted by the fibre is dependent on the strength of the fibre and on the effectiveness of the anchorage of the ends of the fibre. A *perfectly plastic* limiting value of fibre stress may be reached either permanently, because the fibre is pulling out at constant stress (Fig. 13a), or temporarily, because the fibre itself has an extended ductile region of extension from a yield strain ε_{fy} to a breakage strain $\varepsilon_{fb} = \kappa \varepsilon_{fy}$ (Fig. 6b).

The second asymptotic possibility is one in which all the fibres have broken to a length (of the order of typical particle size) at which they have no residual bond length (Fig. 13b). Once broken, the fibre force in the infinitesimal element is zero for all subsequent strain increments. However, the fragments of fibre still occupy space in the fibre-soil mixture, and thus, continue to influence the values of specific volume which recognise the presence of the fibres, with or without their attendant voids, v_{sv} (9) and v_s (10).

In principle, infinite strain is needed to reach asymptotic states in which all aspects of fabric and state have stopped changing (Ibraim et al., 2010b). The concept of small strain asymptotic or limiting response is slightly oxymoronic. Typical test apparatus are not capable of applying infinite strains (apart from ring shear (Consoli et al., 2005)): we seek tendencies towards, rather than arrivals at, asymptotic destinations.

Shearing at constant volume implies that the Mohr circle of strain increment is centred on the origin so that all fibres with orientation lying within one sector of $\pi/2$ from the horizontal will be subject to extension stretching strains. The mechanical contribution of the fibres results from the interaction of the fibre orientations with the Mohr's circles of strain increment (Fig. 4). As a simple illustration, suppose that the fibres are uniformly distributed across all orientations so that $p_\theta = 1/\pi$, and that the fibre/soil sample is being sheared at constant volume. Successive Mohr circles (centred on the origin) are shown in Fig. 14a. Where the tensile strain is less than yield
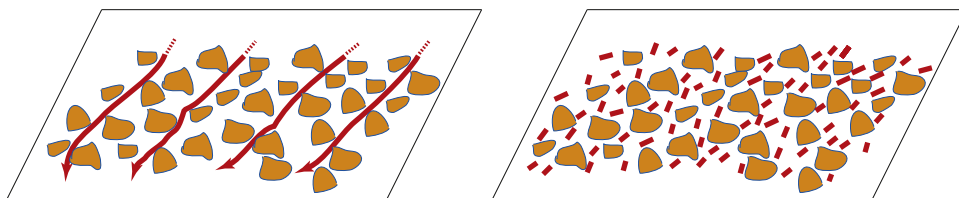

Fig. 13. Asymptotic states for fibre-sand mixtures: (a) fibres continuously pulling through soil; (b) fibres breaking.
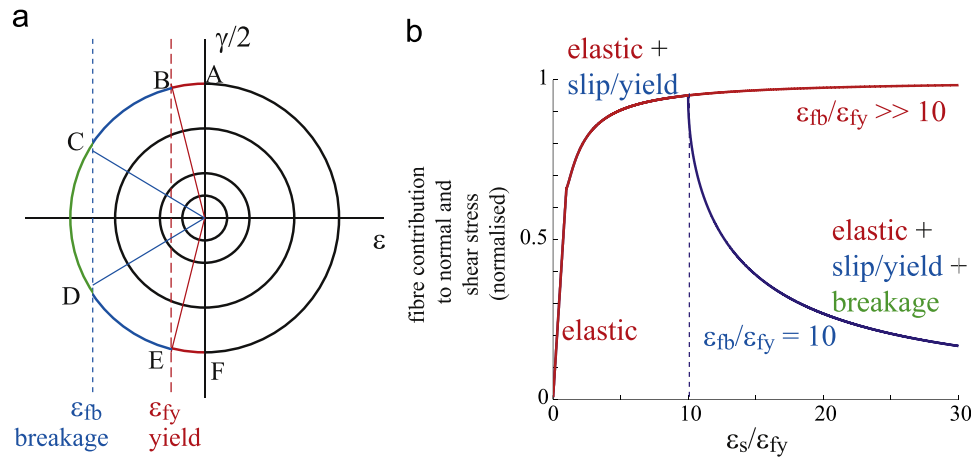
Fig. 14. a. Mohr circles of strain for increasing shearing at constant volume: yield/slip of fibres at tensile strain ε_y; breakage of fibres at tensile strain ε_b (Mohr circle sectors AB and EF: elastic; BC and DE: ductile fibre response, constant P; CD: broken fibres); b. fibre contribution to normal stress and shear stress with increasing shear strain ε_s.
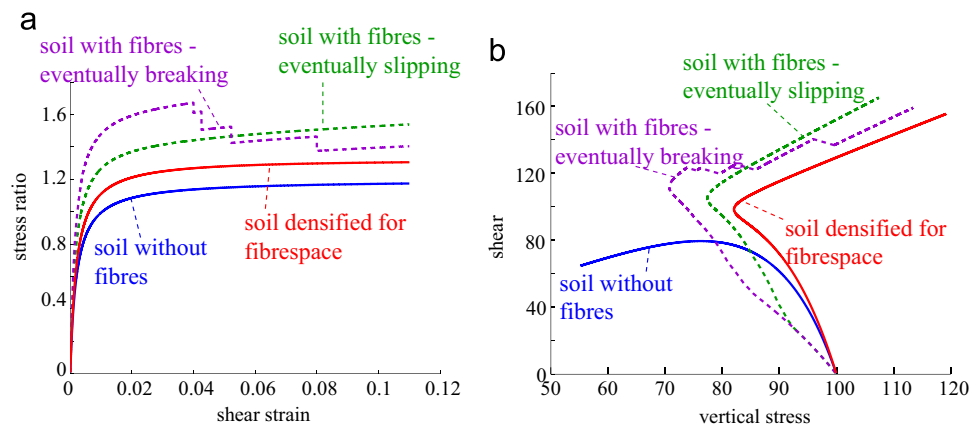

Fig. 15. Simulations of constant volume tests on sand-fibre mixture.

strain ε_y, the fibres are stretched elastically; for tensile strains in the range $\varepsilon_y - \varepsilon_b$, the fibres generate a constant yield or slipping force (Fig. 13a). Where the strain exceeds ε_b, the fibres break (Fig. 13b). The resulting development of fibre contribution with strain is shown in Fig. 14b – it is entirely determined by the Mohr circle of strain (for monotonic shearing).

We can build up the expected constant volume response of an initially loose soil (state parameter $\psi > 0$) to which fibres have been added (Fig. 15). The loose soil on its own wishes to contract as it is sheared in order to approach the critical state. The externally imposed normal stress decreases in order to permit elastic expansion to counter the tendency to contraction. The effective stress path heads towards the origin (Fig. 15b).

Adding in the fibres, the theft of the voids to form fibrespace leaves the soil feeling denser so that the tendency to contract is replaced by a tendency to expand and the vertical stress has to increase to counter this tendency. The stress:strain relationship for the sand alone shows higher stiffness and strength because of the higher perceived density; the effective stress path also shows

dilative tendencies. The vertical stress initially falls, but then rises rapidly in order to counter the desire of the soil to dilate.

However, the fibres being stretched by the shearing want to compress the soil. Therefore, the vertical stress has to decrease in order to keep the volume constant. The eventual stress path for the mixture thus lies to the left of the path for the pseudo-densified soil. The simulations shown here have been performed using a division of orientations into 36 sectors of 5°. The orientations of fibres have been uniformly distributed across these orientations. Consequently, the integrated contributions of the fibres to *increase* in shear stress and to *decrease* in normal stress are of equal magnitude.

With soil-fibre interaction chosen to lead to eventual perfectly plastic pull-through $\varepsilon_{fb} \gg \varepsilon_{fy}$ (Fig. 14b), the stress: strain response and stress path show a sustained benefit from the fibres. With alternative parameters which lead to fibre breakage, the benefit is steadily lost - fibres around $\pi/4$ to the horizontal experience the largest strains and break first (Fig. 14). Fig. 14b indicates the asymptotic responses corresponding to either of these limits. Breakage proceeds around the fibre orientations: the step-wise nature of the curves shown

in Fig. 15 corresponds to this sequential breakage. With complete breakage the fibre-soil mixture reverts to the response of the sand densified by the removal of fibrespace: even with complete breakage, there is some residual benefit compared with the original loose sand (Fig. 15).

Shearing in an asymptotic state must be occurring at constant volume − it would otherwise be unsustainable. In the stress-dilatancy plot of Severn-Trent sand (Fig. 3d), the soil will reach its critical state as usual with mobilised friction corresponding to the critical state stress ratio M. However, the mobilised friction determined externally, $R_{ext} = \tau_{ext}/\sigma_{ext}$, is not the friction mobilised in the soil, $R_s = \tau_s/\sigma_s$. The fibres being stretched provide extra normal stress (σ_f) in addition to that externally applied: $\sigma_s = \sigma_{ext} + \sigma_f$. The fibres also provide some increased shearing resistance beyond that generated in the soil, τ_f. Thus, for the soil, the mobilised friction is

$$R = \frac{\tau_s}{\sigma_s} = \frac{\tau_s}{\sigma_{ext} + \sigma_f} = \frac{\tau_s}{\sigma_{zs}} \qquad (11)$$

reaching value M at the critical state. The externally determined mobilised friction is

$$R_{ext} = \frac{\tau_{ext}}{\sigma_{ext}} = \frac{\tau_s + \tau_f}{\sigma_{ext}} = \frac{\tau_s + \tau_f}{\sigma_s - \sigma_f} \qquad (12)$$

More to the point, the routes by which the soil resistance and the contributions of the fibres are generated are quite different. The stress-dilatancy plot (Fig. 3d) forms part of the description of the soil based on our experience of the elastic-plastic constitutive modelling of soils. The presence of the fibres appears to push the stress-dilatancy plot away from the critical state for the soil alone. However, we have two contributions − fibre and soil − which are responding mechanically in quite different ways and the pattern appropriate for one is not relevant for the other.

5. Roots

Much of our discussion has been generic so far as the nature of the flexible elements within the soil is concerned. For our polypropylene fibres of uniform cross-section and length, it is essential to know the distribution and orientation of the fibres. That necessity remains with the roots, but the variability in dimensions and mechanical properties must be added. Fibre bundle or root bundle models (Pollen and Simon, 2005; Mickovski et al., 2009; Schwarz et al., 2010a) provide a structured means of describing such variability. In most models, roots have been considered as very flexible elements, like our fibres, appropriate for the finest roots. 'Structural roots' with significant flexural resistance require a different sort of modelling (Reubens et al., 2007) − but also reflect different plant species which may be less appropriate for general soil improvement. Roots may have different failure mechanisms, can break or pull-out, while the length, apparent Young's modulus, and maximum tensile force are functions of root diameter and age (Schwarz et al., 2010b). Root tortuosity can affect the root stiffness (Schwarz et al., 2011); root topology, branching angle, and branching density can significantly change the distribution of stresses and plastic strains within the soil (Stokes et al., 1996; Mickovski et al., 2007; Dupuy et al., 2005; Loades et al., 2010; Danjon and Reubens, 2008; Mickovski and van Beek, 2009). However, some of these effects relate to the soil-root system - moving up a scale from the 'infinitesimal' continuum element that has been our focus.

6. Conclusion

We have developed a framework for modelling the interaction of soil with flexible fibres. The mechanics of the individual components − soil and fibres − are not changed in their combination, but it is their interaction which provides a greater challenge. It is obvious that, whatever the nature of the flexible inclusions, it will be necessary to know their distribution, orientation, dimensions, and mechanical properties if we are to have some hope of being able to produce successful simulations.

Part of the description of the interaction between soil and fibres relates to the appropriate choice of description of the packing of the mixture. The concept of stolen void ratio or fibrespace has been invoked in order to be able to describe the significant changes in dilatancy, which imply a reduction in state parameter, in the presence of the fibres. The consequences of fibrespace require further exploration concerning both the physical justification and the potential for evolution with shearing or increased stress.

There are several different ways in which the volumetric proportions of different constituents in a mixture can be described. Basing an assessment of comparative response on one description rather than another is hardly conclusive. The gathering of completely defined experimental observations can most usefully be fed into the parallel process of model development.

The interaction of soils with flexible fibres − or roots − can be simulated rather satisfactorily with appropriate allowance for the volumes occupied or demanded by the several phases. The test observations and the elements of the modelling for the soil and for the soil-fibre mixtures demonstrate once again the importance of considering volume and density change in soils in parallel with changes in effective stress − reinforcing the underpinning message of critical state soil mechanics.

References

Batdorf, S., Budiansky, B., 1949. A mathematical theory of plasticity based on the theory of slip. Technical note 1871, NACA.

Been, K., Jefferies, M., 1985. A state parameter for sands. Géotechnique 35 (2), 99–112.

Calladine, C., 1971. A microstructural view of the mechanical properties of a saturated clay. Géotechnique 21 (4), 391–415.

Chang, C., Hicher, P.-Y., 2005. An elastic-plastic model for granular materials with microstructural consideration. Int. J. Solids Struct. 42 (14), 4258–4277.

Consoli, N., Casagrande, Dal Toe, Coop, M, M., 2005. Effect of fibre reinforcement on the isotropic compression behaviour of a sand. J. Geotech. Geoenviron. Eng. ASCE 131 (11), 1434–1436.

Cox, H.L., 1952. The elasticity and strength of paper and other fibrous materials. Br. J. Appl. Phys. 3 (3), 72–79.

Danjon, F., Reubens, N., 2008. Assessing and analyzing 3D architecture of woody root systems, a review of methods and applications in tree and soil stability, resource acquisition and allocation. Plant Soil 303 (1), 1–34.

di Prisco, C., Nova, R., 1993. A constitutive model for soil reinforced by continuous threads. Geotext. Geomembr. 12 (2), 161–178.

Diambra, A., Ibraim, E., 2014. Modelling of fibre cohesive soil mixtures. Acta Geotech. 9 (6), 1029–1043. http://dx.doi.org/10.1007/s11440-013-0283-y.

Diambra, A., Ibraim, E., 2015. Fibre-reinforced sand: interaction at the fibre and grain scale. Géotechnique 65 (4), 296–308. http://dx.doi.org/10.1680/geot.14.P.206.

Diambra, A., Ibraim, E., Muir Wood, D., Russell, A.R., 2010. Fibre reinforced sands: experiments and modelling. Geotext. Geomembr. 28 (3), 238–250. http://dx.doi.org/10.1016/j.geotexmem.2009.09.010.

Diambra, A., Ibraim, E., Russell, A.R., Muir Wood, D., 2011. Modelling the undrained response of fibre reinforced sands. Soils Found. 51 (4), 625–636. http://dx.doi.org/10.3208/sandf.51.625.

Diambra, A., Ibraim, E., Russell, A.R., Muir Wood, D., 2013. Fibre reinforced sands: from experiments to modelling and beyond. Int. J. Numer. Anal. Methods Geomech. 37 (15), 2427–2455. http://dx.doi.org/10.1002/nag.2142.

Diambra, A., Russell, A.R., Ibraim, E., Muir Wood, D., 2007. Determination of fibre orientation in reinforced sands. Géotechnique 57 (7), 623–628. http://dx.doi.org/10.1680/geot.2007.57.7.623.

Ding, D., Hargrove, S., 2006. Nonlinear stress-strain relationship of soil reinforced with flexible geofibers. J. Geotech. Geoenviron. Eng. ASCE 132 (6), 791–794.

Dupuy, L., Fourcaud, T., Stokes, A., 2005. A numerical investigation into factors affecting the anchorage of roots in tension. Eur. J. Soil Sci. 56, 319–327.

Gajo, A., Muir Wood, D., 1999a. A kinematic hardening constitutive model for sands: the multiaxial formulation. Int. J. Numer. Anal. Methods Geomech. 23 (5), 925–965.

Gajo, A., Muir Wood, D., 1999b. Severn-Trent sand: a kinematic hardening constitutive model for sands: the $q - p$ formulation. Géotechnique 49 (5), 595–614.

Gudehus, G., 1997. Attractors, percolation thresholds and phase limits of granular soils. Behringer, R., Jenkins, J. (Eds.), Powders and Grains, 97. Balkema, Rotterdam, pp. 169–183.

Heineck, K.S., Coop, M.R., Consoli, N.C., 2005. Effect of microreinforcement of soils from very small to large shear strains. J. Geotech. Geoenviron. Eng. ASCE 131 (8), 1024–1033.

Hull, D., Clyne, T.W., 1996. An introduction to composite materials Cambridge Solid State Science Series. 2nd Edition Cambridge University Press.

Ibraim, E., Diambra, A., Russell, A.R., Muir Wood, D., 2012. Assessment of laboratory sample preparation for fibre reinforced sands. Geotext. Geomembr. 34, 69–79. http://dx.doi.org/10.1016/j.geotexmem.2012.03.002.

Ibraim, E., Diambra, A., Muir Wood, D., Russell, A.R., 2010a. Static liquefaction of fibre reinforced sand under monotonic loading. Geotext. Geomembr. 28 (4), 374–385. http://dx.doi.org/10.1016/j.geotexmem.2009.12.001.

Ibraim, E., Fourmont, S., 2007. Behaviour of sand reinforced with fibres. In: Ling, H. I., Callisto, L., Leshchinsky, D., Koseki, J. (Eds.), Soil Stress–Strain Behaviour: Measurement, Modelling and Analysis: Geotechnical Symposium in Roma. Springer, pp. 807–918 (http://dx.doi.org/10.1007/978-1-4020-6146-2_60).

Ibraim, E., Lanier, J., Muir Wood, D., Viggiani, G., 2010b. Strain path controlled shear tests on an analogue granular material. Géotechnique 60 (7), 545–559. http://dx.doi.org/10.1680/geot.8.P.100.

Ibraim, E., Maeda, K., 2007. Numerical analysis of fibre-reinforced granular soils. In: Otani, J., Miyata, Y., Mukunoki, T. (Eds.), New horizons in earth reinforcement, Proceedings of 5th International Symposium on Earth Reinforcement, IS Kyushu '07. Balkema, Rotterdam, pp. 387–393.

Ibraim, E., Muir Wood, D., Maeda, K., Hirabayashi, H., 2006. Fibre-reinforced granular soils behaviour: numerical approach. In: Hyodo, E.M., Murata, H., Nakata, Y. (Eds.), Proceedings of the International Symposium on Geomechanics and Geotechnics of Particulate Media. Taylor & Francis Group, pp. 443–448.

Jewell, R.A., Wroth, C.P., 1987. Direct shear tests on reinforced sand. Géotechnique 37 (1), 53–68.

Kutschera, L., Lichtenegger, E., Sobotik, M., 1960–2009. Wurzelatlas. DLG-Verlag/Gustav Fischer Verlag/Leopold Stocker Verlag.

Li, C., Zornberg, J.G., 2013. Mobilization of reinforcement forces in fiber reinforced soil. J. Geotech. Geoenviron. Eng. ASCE 139, 107–115.

Liang, T., 2016. Personal communication.

Lirer, S., Flora, A., Consoli, N.C., 2011. On the strength of fibre-reinforced soils. Soils Found. 51 (4), 601–609.

Loades, K.W., Bengough, A.G., Bransby, M.F., Hallett, P.D., 2010. Planting density influence on fibrous root reinforcement of soils. Ecol. Eng. 36, 276–284.

Maher, M., Gray, D., 1990. Static response of sand reinforced with fibres. J. Geotech. Eng. ASCE 116 (11), 1661–1677.

Michałowski, R., Čermák, J., 2002. Strength anisotropy of fiber-reinforced sand. Comput. Geotech. 29 (4), 279–299.

Michałowski, R.L., Čermák, J., 2003. Triaxial compression of sand reinforced with fibers. J. Geotech. Geoenviron. Eng. ASCE 129 (2), 125–136.

Mickovski, S., Bengough, A., Bransby, M., Davies, M., Hallett, P., Sonnenberg, R., 2007. Material stiffness, branching pattern and soil matric potential affect the pullout resistance of model root systems. Eur. J. Soil Sci. 58, 1471–1481.

Mickovski, S., Hallett, P., Bransby, M., Davies, M., Sonnenberg, R., Bengough, A.G., 2009. Mechanical reinforcement of soil by willow roots: impacts of root properties and root failure mechanism. J. Soil Sci. Soc. Am. 73, 1276–1285.

Mickovski, S., van Beek, L., 2009. Root morphology and soil reinforcement effects of young vetiver (*Vetiveria zizanioides*) plants grown in a semi-arid climate. Plant Soil 324 (1), 43–56.

Muir Wood, D., 2009. Soil Mechanics: a One-dimensional Introduction. Cambridge University Press.

Muir Wood, D., 2012. Soils in space. In: Yang, Q., Zhang, J.-M., Zheng, H., Yao, Y. (Eds.), Constitutive Modelling of Geomaterials: Advances and New Applications. Springer, pp. 239–246.

Muir Wood, D., Diambra, A., Ibraim, E., 2014. Fibres and roots for soil improvement. Soga, K., Kumar, K., Biscontin, G., Kuo, M. (Eds.), Geomechanics from Micro to Macro, Vol. 2. CRC Press, Taylor and Francis Group, pp. 1503–1508.

Pande, G., Sharma, K., 1983. Multi-laminate model of clays: a numerical evaluation of the influence of rotation of the principal stress axes. Int. J. Numer. Anal. Methods Geomech. 7 (4), 397–418.

Pollen, N., Simon, A., 2005. Estimating the mechanical effects of riparian vegetation on stream bank stability using a fiber bundle model. Water Resour. Res. (41).

Ranjan, G., Vasan, R., Charan, H., 1996. Probabilistic analysis of randomly distributed fiber-reinforced soil. J. Geotech. Eng. ASCE 122, 419–426.

Reubens, B., Poesen, J., Danjon, F., Geudens, G., Muys, B., 2007. The role of fine and coarse roots in shallow slope stability and soil erosion control with a focus on root system architecture: a review. Trees Struct. Funct. 21 (4), 385–402.

Roscoe, K.H., Schofield, A.N., Wroth, C.P., 1958. On the yielding of soils. Géotechnique 8 (1), 22–52.

Schwarz, M., Cohen, D., Or, D., 2010a. Soil-root mechanical interactions during pullout and failure of root bundles. J. Geophys. Res. 115 (F04035).

Schwarz, M., Cohen, D., Or, D., 2011. Pullout tests of root analogs and natural root bundles in soil – experiments and modeling. J. Geophys. Res. 116 (F02007).

Schwarz, M., Lehmann, P., Or, D., 2010b. Quantifying lateral root reinforcement in steep slopes – from a bundle of roots to tree stands. Earth Surf. Process. Landforms 35, 354–367.

Silva dos Santos, A., Consoli, N., Baudet, B., 2010. The mechanics of fibre reinforced sand. Géotechnique 60 (10), 791–799.

Stokes, A., Ball, J., Fitter, A., Brain, P., Coutts, M., 1996. An experimental investigation into the resistance of model root systems to uprooting. Ann. Bot. 78, 415–421.

Villard, P., Jouve, P., Riou, Y., 1990. Modélisation du comportement mécanique du Texsol. Bull. Liaison Lab. Ponts Chauss. 68, 15–28.

Wroth, C.P., Bassett, R.H., 1965. A stress-strain relationship for the shearing behaviour of a sand. Géotechnique 15 (1), 32–56.

Wu, T., McOmber, R.M., Erb, R.T., Beal, P.E., 1988. Study of soil-root interaction. J. Geotech. Eng. ASCE 114 (12), 1351–1375.

Zornberg, J., 2002. Discrete framework for equilibrium analysis of fibre reinforced soil. Géotechnique 52 (8), 593–604.